

Fig. S1. Confirmation of cell type-specific infection of lentivirus. (A) Construction of LV-Venus and LV-dnRAR α vectors. (B,C) At day 5 after the injection of LV-Venus, expression of broad germ cell marker TRA98 (magenta) and Venus (Green) were examined with immunohistochemistry. Scale bars: 80 μ m.

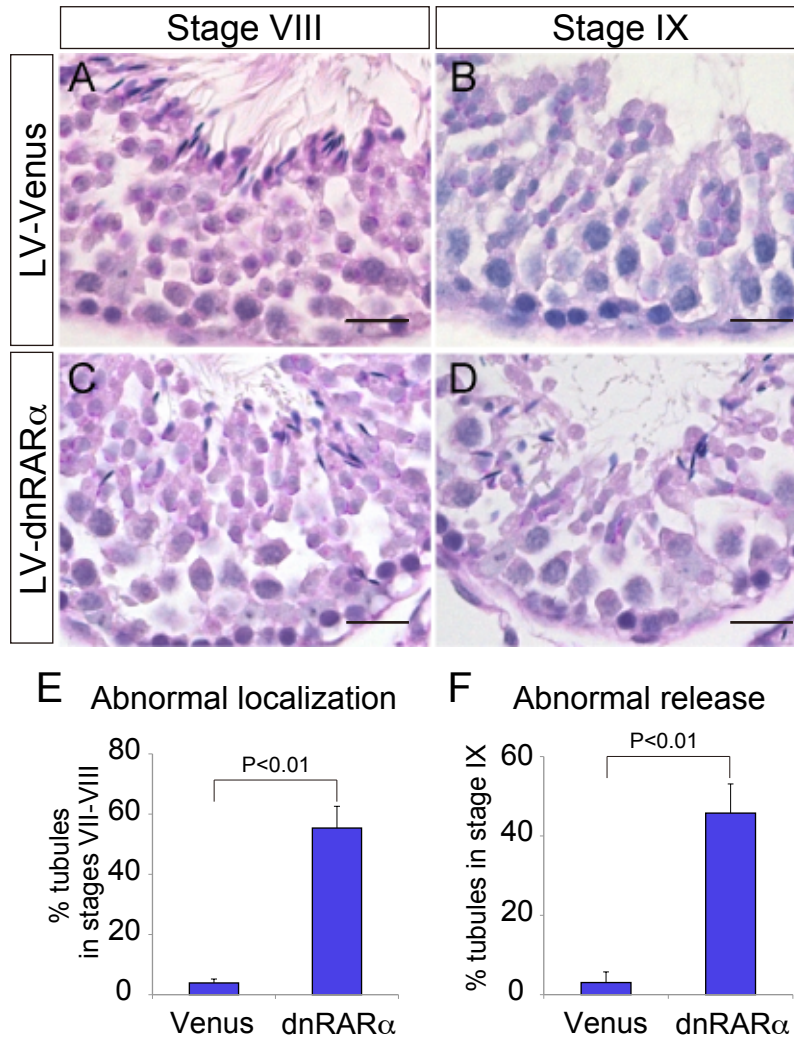


Fig. S2. Abnormal transition and release of elongated spermatids upon the overexpression of dnRAR α . (A-D) Histological sections derived from mouse testes injected with LV-Venus or LV-dnRAR α at stage VIII or stage IX. (E) Proportion of Venus-positive tubules at stages VII-VIII showing abnormal alignment of elongated spermatids ($n=4$). (F) Proportion of Venus-positive tubules at stage IX containing abnormally retained elongated spermatids ($n=4$). Only Venus-positive tubules were counted. Error bars, s.d. Scale bars: 20 μ m.

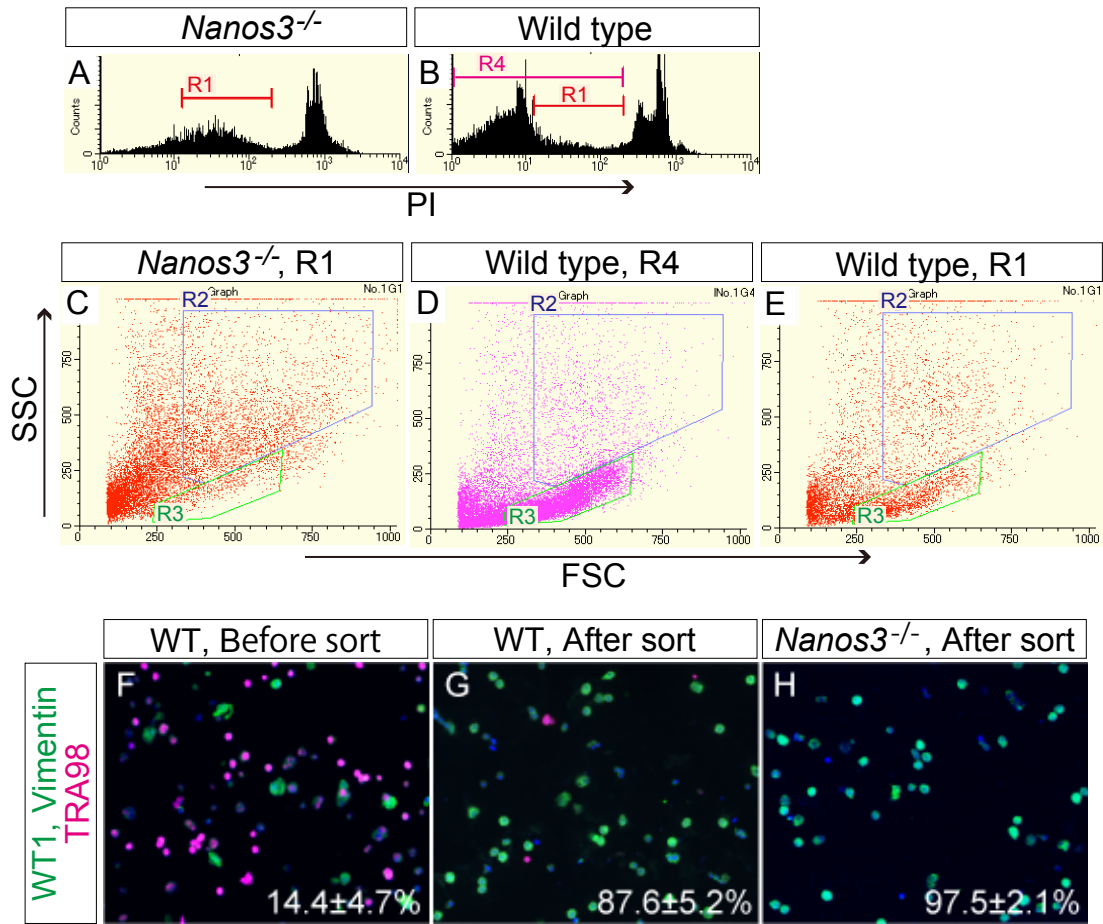


Fig. S3. Direct isolation of Sertoli cells from adult testes by FACS. (A,B) Testicular cells obtained from *Nanos3*^{-/-} or wild-type mice were analyzed by FACS. Propidium iodide (PI)-negative cells (R4) or cells showing high intrinsic fluorescence (R1) were selected for flow sorting. PI-positive dead cells were removed. (C-E) R1 fractions from *Nanos3*^{-/-} or wild-type testicular cells and an R4 fraction from wild-type testicular cells. R2 and R3 fractions represent Sertoli cells and germ cells, respectively. (F-H) Wild-type testicular cells before and after sorting and *Nanos3*^{-/-} testicular cells after sorting were immunostained with antibodies against WT1, vimentin (green) and TRA98 (magenta). The proportions of WT1 and vimentin-positive Sertoli cells are indicated at the bottom-right of the lower panels. The values are the mean ± s.d.

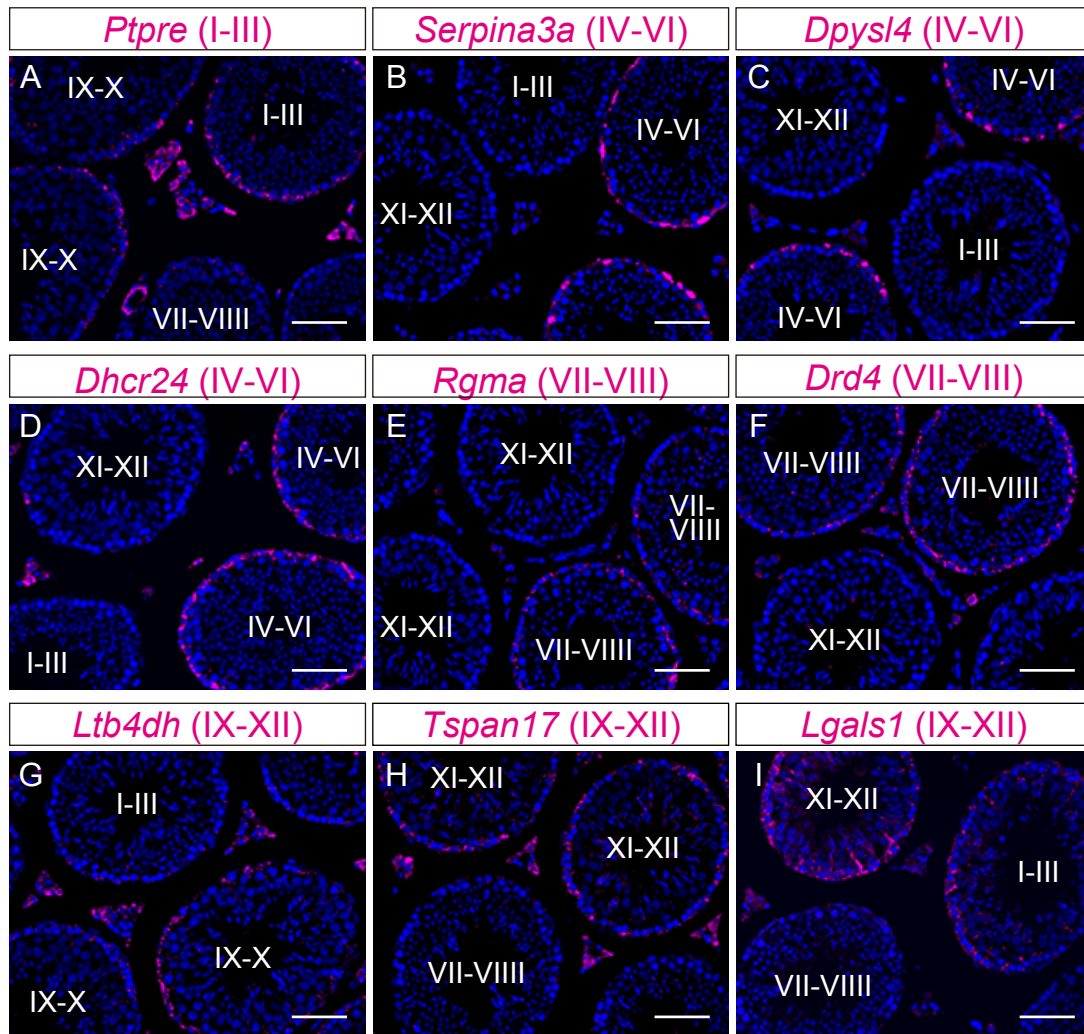


Fig. S4. Validation of the microarray results. (A-I) The spatial expression patterns of nine genes identified as stage-dependent and showing peaks during stages I-III (*Ptpre*), IV-VI (*Serpina3a*, *Dpysl4*, *Dhcr24*), VII-VIII (*Rgma*, *Drd4*) and IX-XII (*Ltb4dh*, *Tspan17*, *Lgals1*) were examined by in situ hybridization. The seminiferous epithelial stages were determined by serial section staining with PAS and Hematoxylin. Scale bars: 80 μ m.

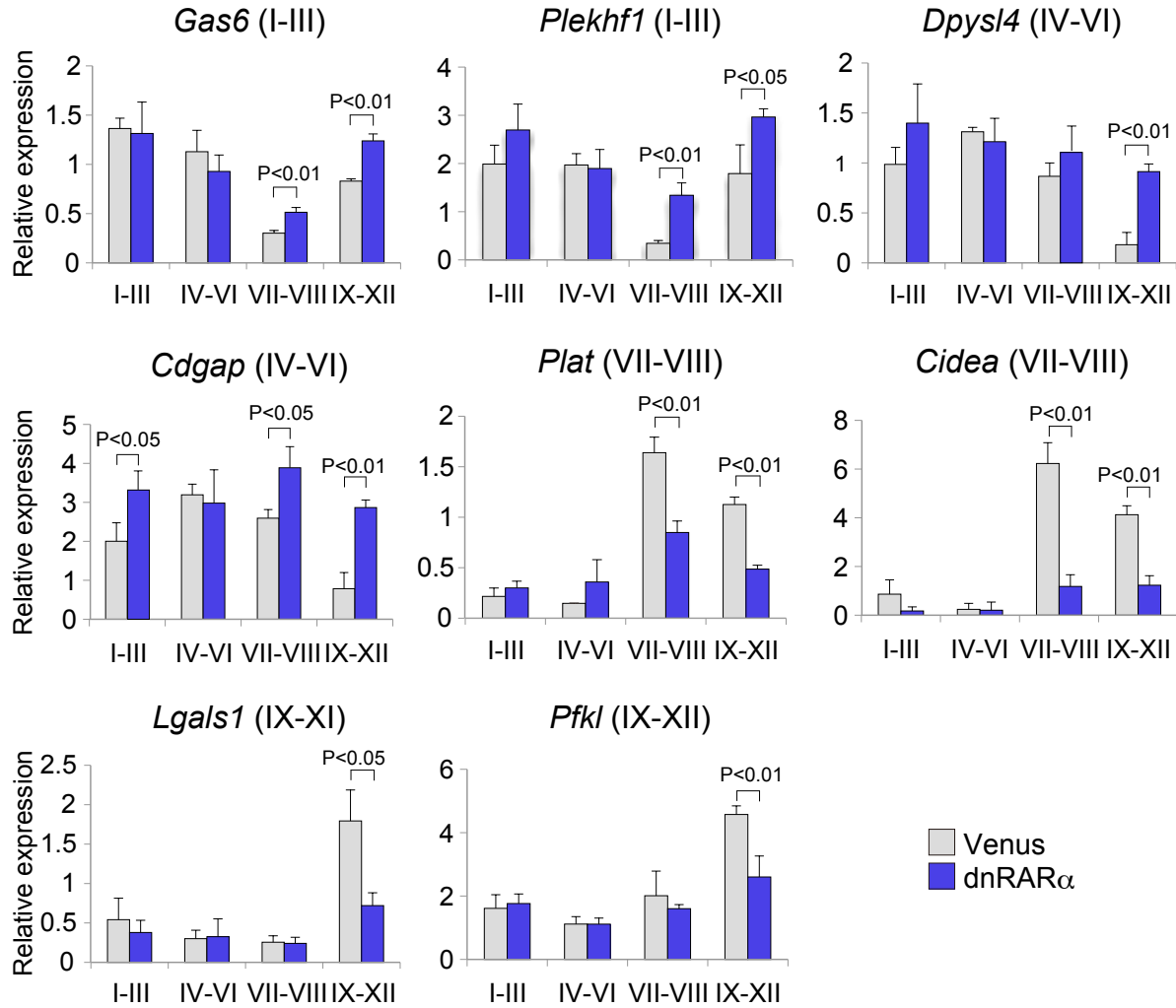


Fig. S5. Validation of the gene expression changes induced by the overexpression of dnRARα. At day 5 after the injection of LV-dnRARα or LV-Venus, stage-specific Venus⁺ tubules were isolated and the expression of the indicated stage-dependent genes showing peaks during stages I-III (*Gas6*, *Plekhf1*), IV-VI (*Dpysl4*, *Cdgap*), VII-VIII (*Plat*, *Cidea*) and IX-XII (*Lgals1*, *Pfk1*) were quantified by qRT-PCR ($n=3$). *Gapdh* was used as internal control. Error bars, s.d.

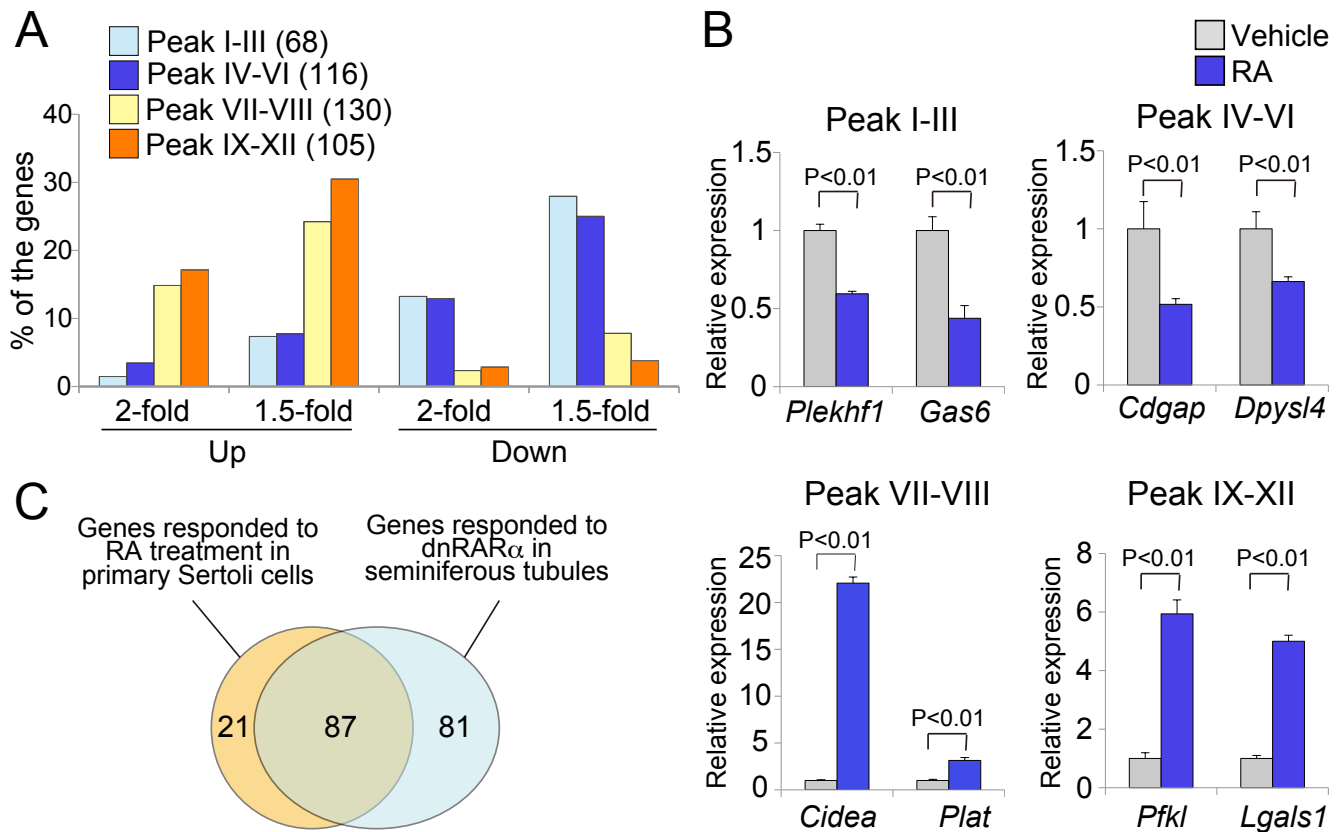


Fig. S6. Expression changes of the stage-dependent genes upon the activation of RA signaling in primary Sertoli cells. (A) Cultured Sertoli cells were incubated with 1 μ M RA for 24 hours and the expression changes of stage-dependent genes were measured by microarray ($n=2$). y -axis represents total percentage of genes that showed up- or downregulation. (B) To validate the microarray results, the expression of stage-dependent genes showing peaks during stages I-III (*Plekhhf*, *Gas6*), IV-VI (*Cdgap*, *Dpysl4*), VII-VIII (*Cidea*, *Plat*) and IX-XII (*Pfk1*, *Lgals1*) in cultured Sertoli cells treated with RA were quantified using qRT-PCR ($n=3$). *Gapdh* was used as internal control. Error bars, s.d. (C) Comparison of genes that responded to RA treatment in primary Sertoli cells (108 genes) and to overexpression of dnRAR α in seminiferous tubules (168 genes). Between those, 87 genes were common.

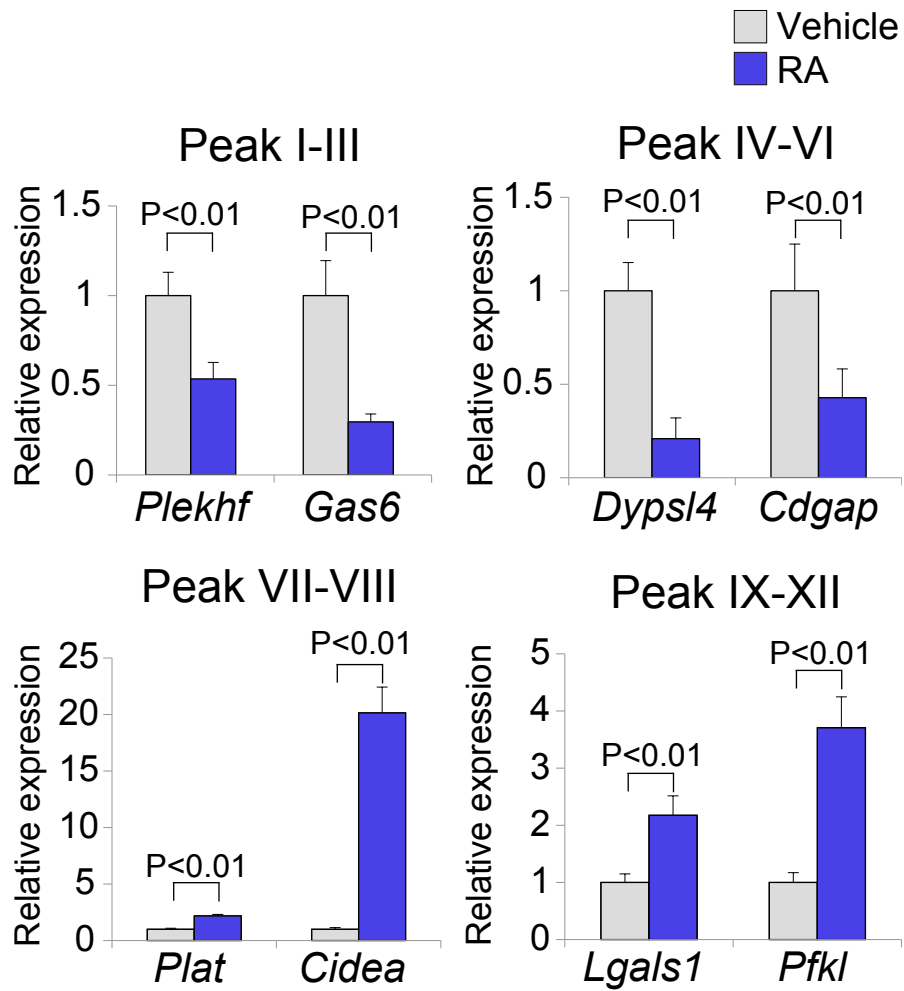


Fig. S7. Expression changes of stage-dependent genes in VAD mice following retinol injections. At 24 hours post-injection, genes showing peak expression during stages I-III (*Plekhf1*, *Gas6*), IV-VI (*Dypsl4*, *Cdgap*), VII-VIII (*Plat*, *Cidea*) and IX-XII (*Lgals1*, *Pfkl*) in whole mouse testes were assayed by qRT-PCR ($n=3$). *Gapdh* was used as internal control. Error bars, s.d.

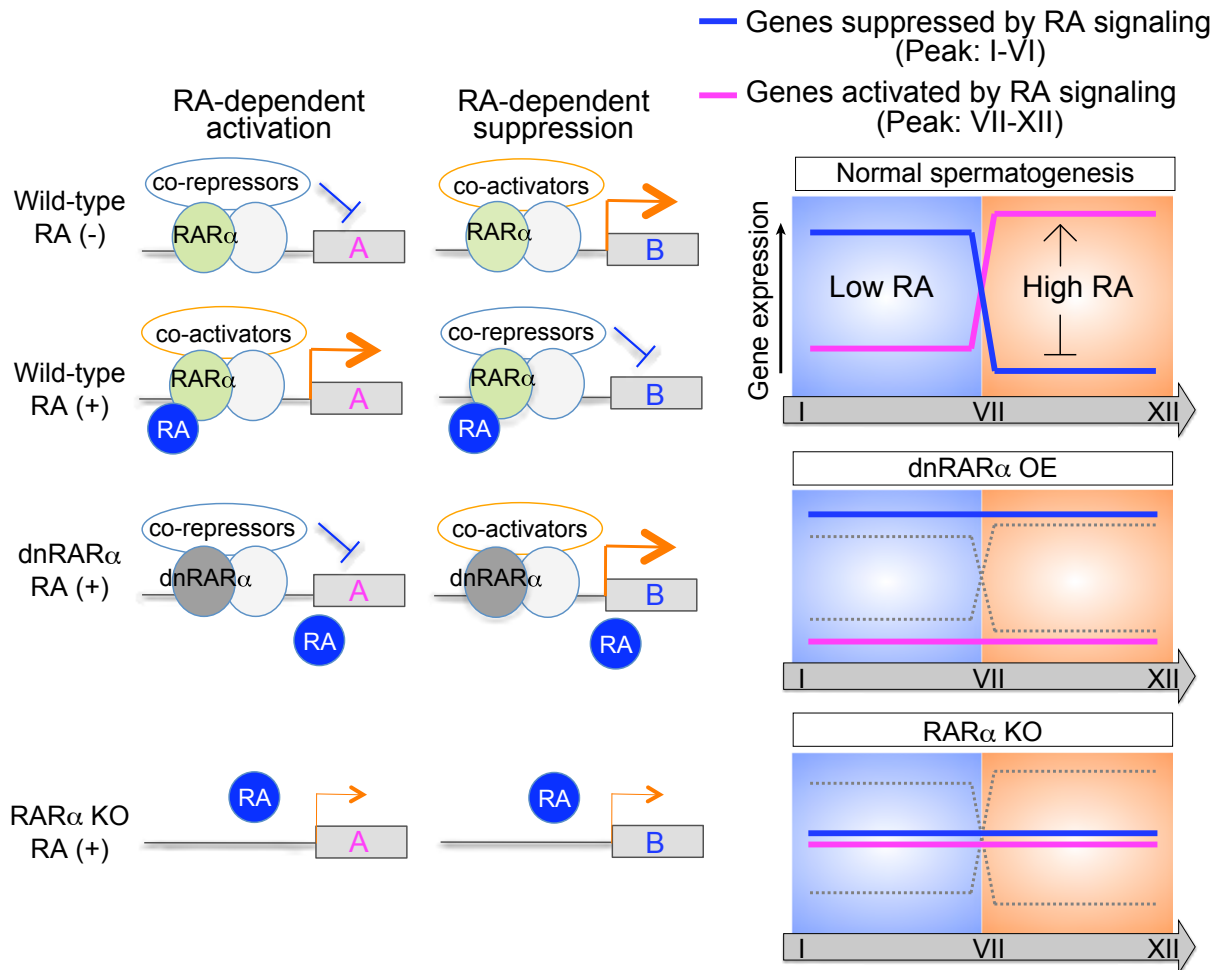


Fig. S8. Proposed model for regulation of stage-dependent gene expression in Sertoli cells by RA signaling. RAR α usually binds to DNA and activates or suppresses the corresponding target genes, even in the absence of RA. Upon the binding of RA, RAR α exchanges the co-regulators and alters the transcription status of the target genes. During normal spermatogenesis, RA signaling is maintained at low and high levels during stages I-VI and VII-XII, respectively, and thereby creates two patterns of gene expression in Sertoli cells through the regulation of RA-responsive genes. Genes suppressed and activated after the binding of RA to RAR α show expression peaks during stages I-VI and VII-XII, respectively. In the case of the overexpression (OE) of dnRAR α , the exchange of co-regulators would not occur even in the presence of RA. As a result, the genes controlled by RA signaling will remain in a stage I-VI-like expression state. In the case of a RAR α KO, both RA-dependent and -independent activation or suppression might be diminished.

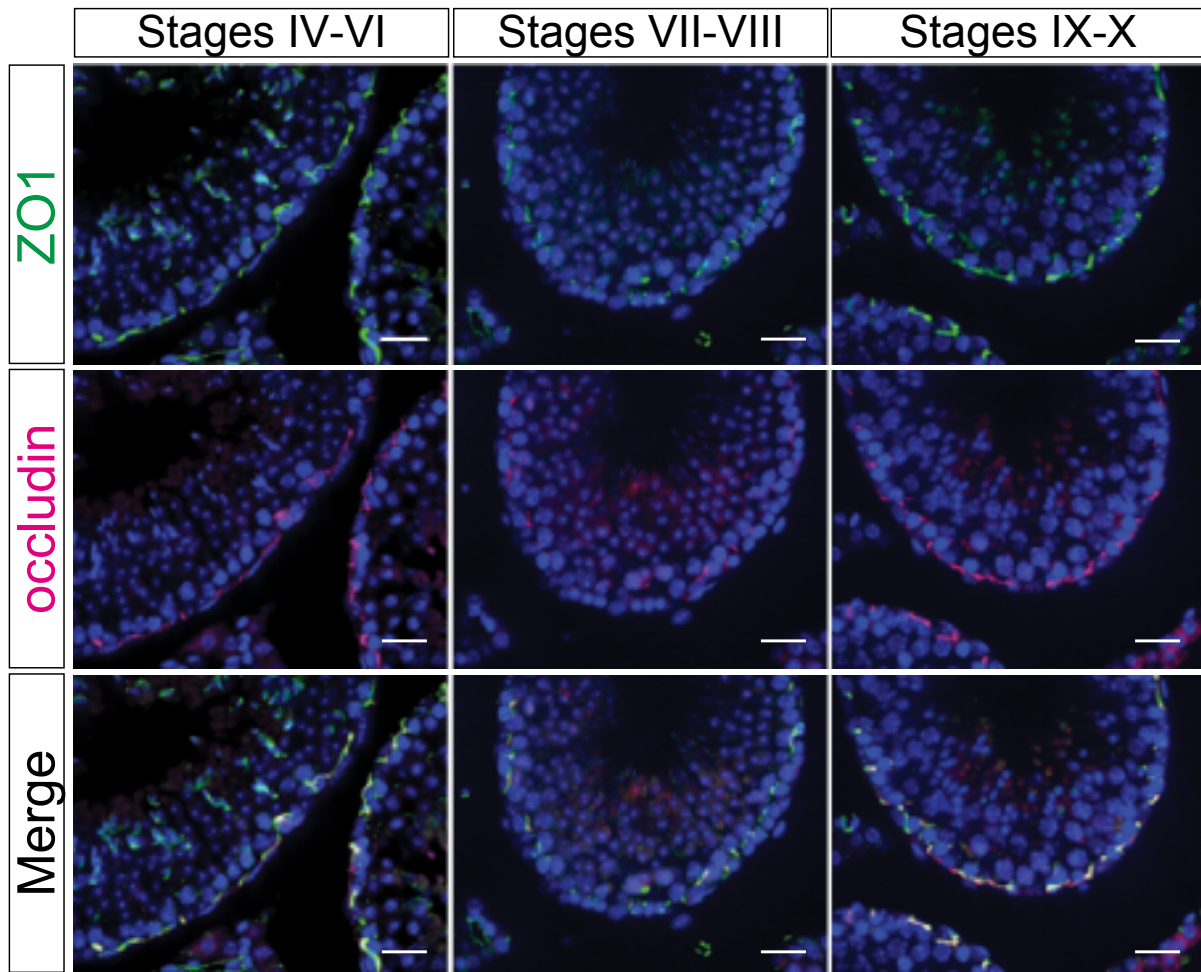


Fig. S9. Stage-dependent expression change of occludin. Immunostaining for ZO1 (green) and occludin (magenta) in stage-specific tubules. Seminiferous epithelial stages were determined with serial sections with PAS and Hematoxylin. Scale bars: 20 μ m.

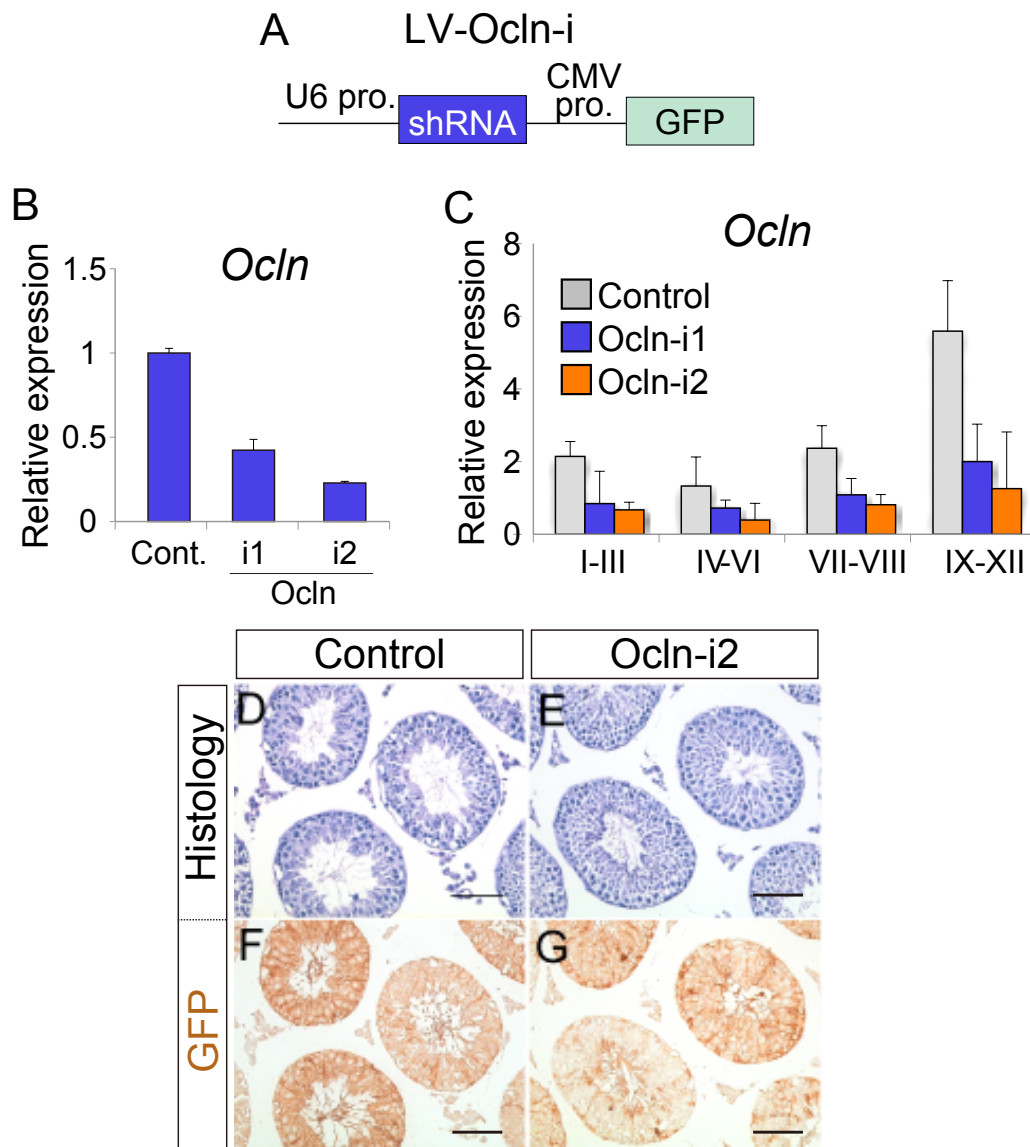


Fig. S10. Efficiency of RNAi in suppressing *Ocln* expression. (A) Construction of the LV-Ocln-i vector. Cells infected with this lentiviral construct start to express both shRNA from the U6 promoter and GFP from the CMV promoter. (B) Cultured Sertoli cells were infected with LV-Ocln-i1 or -i2 and the expression of *Ocln* was subsequently quantified by qRT-PCR ($n=3$). (C) Adult mouse testes were injected with LV-Ocln-i1 or i2 and changes in the stage-dependent expression of *Ocln* were then quantified by qRT-PCR ($n=3$). *Gapdh* was used as internal control. (D-G) Histological analysis of mouse testes at two weeks after injection of LV-control or LV-Ocln-i2 vectors. Tissue sections were stained with PAS and Hematoxylin. Error bars, s.d. Scale bars: 40 μ m.